Electronic Supplementary Material (ESI) for Journal of Materials Chemistry A.

Interface-Engineered Hematite Nanocones as Binder-Free Electrode for High-Performance Lithium-Ion Batteries

Lei Wang,[a,†] Kun Liang,[b,†] Guanzhi Wang,[b] and Yang Yang [b*]

[a] *State Key Laboratory for Oxo Synthesis and Selective Oxidation, National Engineering Research Center for Fine Petrochemical Intermediates, Lanzhou Institute of Chemical Physics, Chinese Academy of Sciences, 730000 Lanzhou, China.*

[b] *NanoScience Technology Center, Department of Materials Science & Engineering, University of Central Florida, 4000 Central Florida Blvd. Orlando, Florida, 32816, United States. E-mail: Yang.Yang@ucf.edu*

†*The authors contributed equally to this work.*

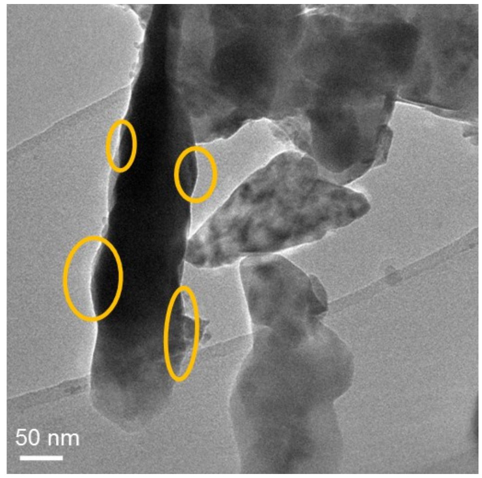

Figure S1. TEM image of Fe_2O_3 NCs with a knoblike structure on the surface.

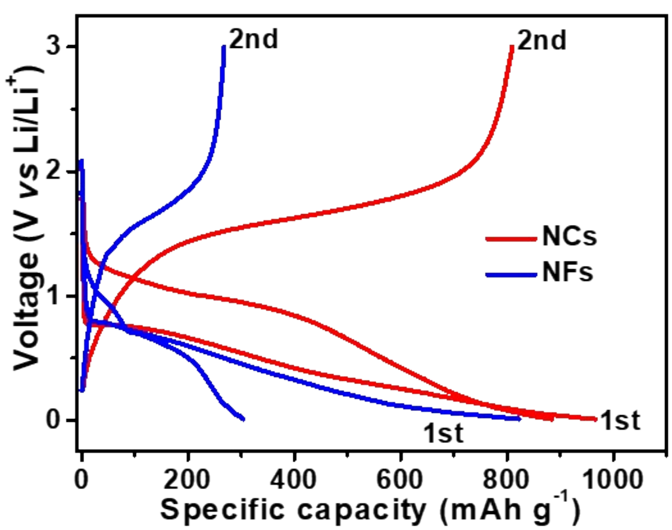

Figure S2. The first two discharge/charge cycling profiles of NCs and NFs at a current density of 0.125 A g^{-1}.

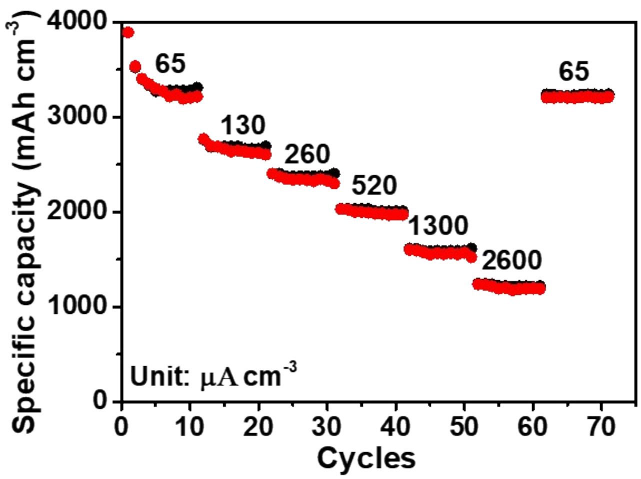

Figure S3. Rate performance.

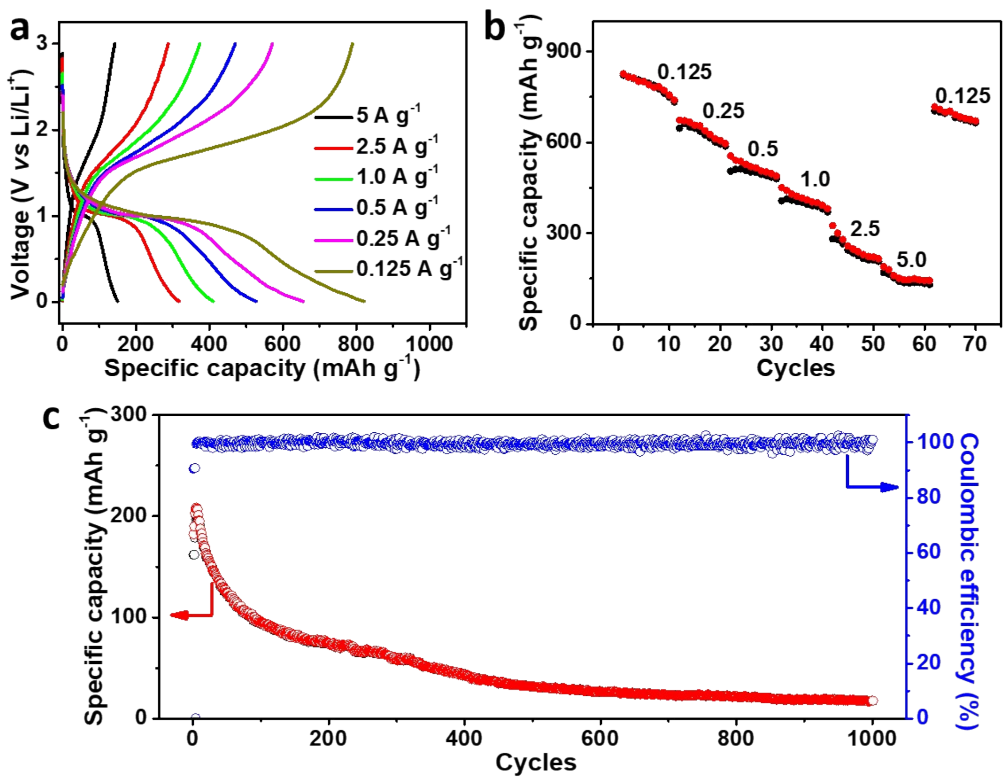

Figure S4. Electrochemical performance of NFs electrode. (a) Charge-discharge profiles at different current densities. (b) Rate performance. (c) Long-term cyclability at a current density of 5 A g^{-1}.

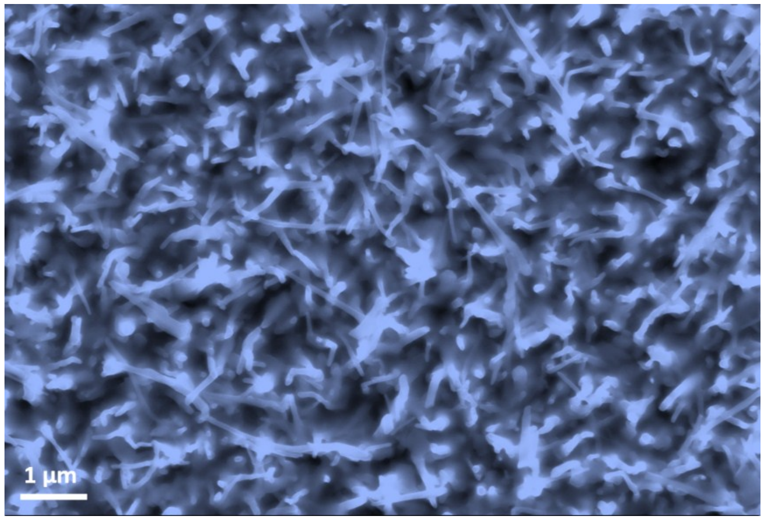

Figure S5. SEM image of NCs electrode after long-term cycling test.

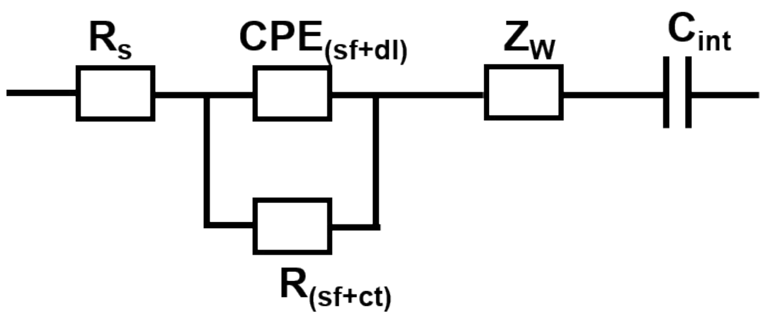

Figure S6. Equivalent electric circuit. The interception at the real axis in the high-frequency area means solution resistance (R_s), which reflects the total resistance between electrolyte and electrode. The diameter of the semicircle or quasi-semicircle in medium frequency combines two resistances, involving Li-ion migration resistance (R_{sf}) and charge-transfer resistance (R_{ct}). The straight line in the low-frequency region represents the Warburg impedance (Z_w), corresponding to Lithium-ion diffusion in the solid.

Table S1. Comparison with the state-of-the-art Fe_2O_3 anodes.

Anode materials	Current density	Specific capacity (mAh g^{-1})	Areal capacity (mAh cm^{-2})	Volumetric capacity (mAh cm^{-3})	Reference
α-Fe_2O_3 NCs	0.125 A g^{-1}	968	0.774	3872	This work
Fe_2O_3/Fe_3C-graphene	50 µA cm^{-2}	-	0.427	3560	1
α-Fe_2O_3 nanoflakes	68 mA g^{-1}	680±20	-	-	2
α-Fe_2O_3 @CNF	50 mA g^{-1}	604	-	-	3
Fe_2O_3-C	1.0 A g^{-1}	812	-	-	4
Fe_2O_3@PANI	0.1 C	893	-	-	5
Graphene- Fe_2O_3	160 mA g^{-1}	660	-	-	6
Fe_2O_3 nanorod-C	0.2 C	758	-	-	7
α-Fe_2O_3-C	0.2 C	688	-	-	8
α-Fe_2O_3	1C	-	0.3831	-	9
C-α-Fe_2O_3	5.04 A g^{-1}	420	0.557	-	10
Fe_2O_3	270 mA g^{-1}	-	-	570	11
Fe_2O_3-graphite	200 mA g^{-1}	-	-	1014	12
Fe_2O_3 NPs	50 µA cm^{-2}	-	-	800	13

Reference

1. Yang, Y.; Fan, X.; Casillas, G.; Peng, Z.; Ruan, G.; Wang, G.; Yacaman, M. J.; Tour, J. M., Three-Dimensional Nanoporous Fe_2O_3/Fe_3C-Graphene Heterogeneous Thin Films for Lithium-Ion Batteries. *ACS Nano* **2014,** *8* (4), 3939-3946.

2. Reddy, M.; Yu, T.; Sow, C.-H.; Shen, Z. X.; Lim, C. T.; Subba Rao, G.; Chowdari, B., α-Fe_2O_3 nanoflakes as an anode material for Li-ion batteries. *Advanced Functional Materials* **2007,** *17* (15), 2792-2799.

3. Ji, L.; Toprakci, O.; Alcoutlabi, M.; Yao, Y.; Li, Y.; Zhang, S.; Guo, B.; Lin, Z.; Zhang, X., α-Fe_2O_3 nanoparticle-loaded carbon nanofibers as stable and high-capacity anodes for rechargeable lithium-ion batteries. *ACS Applied Materials & Interfaces* **2012,** *4* (5), 2672-2679.

4. Cho, J. S.; Hong, Y. J.; Kang, Y. C., Design and synthesis of bubble-nanorod-structured Fe_2O_3–carbon nanofibers as advanced anode material for Li-ion batteries. *ACS Nano* **2015,** *9* (4), 4026-4035.

5. Jeong, J. M.; Choi, B. G.; Lee, S. C.; Lee, K. G.; Chang, S. J.; Han, Y. K.; Lee, Y. B.; Lee, H. U.; Kwon, S.; Lee, G., Hierarchical hollow spheres of Fe_2O_3@polyaniline for lithium ion battery anodes. *Advanced Materials* **2013,** *25* (43), 6250-6255.

6. Wu, Z.-S.; Zhou, G.; Yin, L.-C.; Ren, W.; Li, F.; Cheng, H.-M., Graphene/metal oxide composite electrode materials for energy storage. *Nano Energy* **2012,** *1* (1), 107-131.

7. Liu, Z.; Tay, S. W., Direct growth Fe_2O_3 nanorods on carbon fibers as anode materials for lithium ion batteries. *Materials Letters* **2012,** *72*, 74-77.

8. Cheng, F.; Huang, K.; Liu, S.; Liu, J.; Deng, R., Surfactant carbonization to synthesize pseudocubic α-Fe_2O_3/C nanocomposite and its electrochemical performance in lithium-ion batteries. *Electrochimica Acta* **2011,** *56* (16), 5593-5598.

9. Cao, K.; Jiao, L.; Liu, H.; Liu, Y.; Wang, Y.; Guo, Z.; Yuan, H., 3D Hierarchical Porous α-Fe_2O_3 Nanosheets for High-Performance Lithium-Ion Batteries. *Advanced Energy Materials* **2015,** *5* (4).

10. Brandt, A.; Balducci, A., Ferrocene as precursor for carbon-coated α-Fe_2O_3 nano-particles for rechargeable lithium batteries. *Journal of Power Sources* **2013,** *230*, 44-49.

11. Wang, L.; Xu, H.; Chen, P.; Zhang, D.; Ding, C.; Chen, C., Electrostatic spray deposition of porous Fe_2O_3 thin films as anode material with improved electrochemical performance for lithium–ion batteries. *Journal of Power Sources* **2009,** *193* (2), 846-850.

12. Wang, Y.; Yang, L.; Hu, R.; Ouyang, L.; Zhu, M., Facile synthesis of Fe_2O_3-graphite composite with stable electrochemical performance as anode material for lithium ion batteries. *Electrochimica Acta* **2014,** *125*, 421-426.

13. Yang, Y.; Peng, Z.; Wang, G.; Ruan, G.; Fan, X.; Li, L.; Fei, H.; Hauge, R. H.; Tour, J. M., Three-dimensional thin film for lithium-ion batteries and supercapacitors. *ACS Nano* **2014,** *8* (7), 7279-7287.